TUNNEL–GROUND INTERACTION ANALYSIS: DISCRETE BEAM–SPRING VS. CONTINUOUS FE MODEL

Elefterija Zlatanović, Vlatko Šešov, Dragan Č. Lukić, Aleksandar Prokić, Marina Trajković-Milenković

For the purpose of studying the soil–tunnel structure interaction, a number of two-dimensional linear numerical analyses has been performed with the aid of the software package ANSYS. The present study employs both discrete beam–spring and continuous FE models, in order to estimate their ability to simulate the soil–structure interaction effects. Since these effects are particularly pronounced during seismic events, the main attention has been focused on dynamic analyses. The earthquake loading is simulated under pure shear conditions and determined by the one-dimensional free-field ground response analysis using the code EERA. Results obtained by simplified dynamic analyses are compared with state-of-practice closed-form elastic solutions and significant factors influencing the tunnel–ground interaction are evaluated. In addition, with the author's aim to develop more realistic and relevant models, effects of initial static conditions are also considered in the analyses.

Keywords: *circular tunnel; continuous FE model; discrete beam–spring model; soil–structure interaction; static and dynamic loads*

Analiza interakcije tunela i tla: diskretni model s oprugama nasuprot kontinuiranom modelu s konačnim elementima

Izvorni znanstveni članak

U cilju istraživanja interakcije tunela s okolnim tlom, provedene su dvodimenzijske linearne numeričke analize primjenom softvera ANSYS. Istraživanja su obuhvatila diskretni model s oprugama i kontinuirani model s konačnim elementima, kako bi se ispitala njihova sposobnost u simuliranju efekata interakcije konstrukcije i tla, s posebnim osvrtom na dinamičke analize, imajući u vidu da su ovi efekti posebice izraženi u seizmičkim uvjetima. Utjecaj potresa, simuliran u uvjetima čistog smika, određen je jednodimenzijskom analizom seizmičkog odgovora tla primjenom softvera EERA. Rezultati dobiveni pojednostavljenim dinamičkim analizama upoređeni su s najčešće primjenjivanim analitičkim rješenjima, uz sagledavanje najznačajnijih faktora koji karakteriziraju interakciju tunelske konstrukcije s okolišem. U cilju razvoja što realnijih i relevantnijih modela, analizama su također obuhvaćeni i početni statički uvjeti.

Ključne riječi: *diskretni model s oprugama; interakcija tunela i tla; kontinuirani model s konačnim elementima; kružni tunel; statičko i dinamičko opterećenje*

1 Introduction

Tunnel structures require very high standards in a sense of their safety, not only from the aspect of the construction process [1], but from the viewpoint of their serviceability as well, particularly in terms of earthquake activity. The soil–structure interaction (SSI) effects should not be omitted in analysis of the dynamic response of tunnel structures, having in mind that the interaction effects between a structure and surrounding medium can result in larger external loading to the structure. A tunnel structure, by its presence, considerably modifies the free-field ground motion, and its seismic response is affected by the combined effects of *kinematic interaction* and *dynamic (inertial) interaction*. The kinematic interaction is recognized to be of the outmost significance, and it stands for the inability of a structure to obey the free-field deformation, as the stiffness of the structure impedes a development of the free-field ground motion. The dynamic interaction is caused by the existence of structural mass that makes the effect of inertial force on the response of the surrounding ground. The effects of seismic impact on the tunnel–ground interaction depend on numerous parameters, such as maximum acceleration, intensity, and duration of the earthquake, the stiffness ratio of the tunnel lining and the surrounding medium, as well as on transmission of the shear stress at the tunnel–ground interface. Simplified solutions generally consider two possible extreme cases: full-slip and no-slip. The *full-slip condition* between the lining and the ground considers equal radial displacements and unequal tangential displacements of the tunnel and the ground at their

interface, meaning that the shear stress transmission at the tunnel–ground interface does not exist. This assumption is commonly used in order to evaluate the maximum values of bending moments and shear forces in the tunnel lining, and is proper only in case of a very soft soil, or a high-intensity earthquake event. The *no-slip condition* considers continuity of stresses and displacements at the conjunctive surface of the structure and the ground, and is adopted in order to obtain the extreme values of the thrust in the tunnel lining. Thus, it is rational to compute both of the extreme cases and apply the more critical one. Nowadays, intensive studies are being performed regarding the influence of interface friction on internal tunnel lining forces due to seismic compressional P-wave and shear S-wave events [2].

The seismic response of circular tunnels has been in a focus of a number of studies. According to Owen and Scholl [3], the seismic wave propagation imposes axial compression/extension, longitudinal bending, and cross-section distortion (ovalisation) of circular tunnels. Among these types of deformations, the ovaling deformation is considered to have the most significant influence on the circular tunnel response under earthquake excitation, resulting predominantly from vertical propagation of the shear (S) waves. Consequently, cycles of additional stress concentrations with alternating compressive and tensile stresses are imposed to the tunnel lining, in which case two critical modes occur: compressive dynamic stresses enlarge the compressive static stresses, thus resulting in a local exceeding of the tunnel liner compressive capacity, and tensile dynamic stresses are higher than the

compressive static stresses, thus inducing the occurrence of the tensile stresses in the lining.

There are various simplified methods for evaluation of the seismically induced ovaling deformation of circular tunnel tubes, which are developed under the assumption of two-dimensional plane-strain condition. The most simple *free-field deformation approach*, proposed by Newmark in 1968 [4] and further developed by St. John and Zahrah in 1987 [5], is based on the theory of wave propagation in an infinite, homogeneous, isotropic, elastic medium, and it does not account for any kind of soil–structure interaction. On the other hand, there are analytical expressions after various authors, such as: Burns and Richard in 1964 [6], Hoeg in 1968 [7], Peck et al. in 1972 [8], Schwartz and Einstein in 1980 [9], Wang in 1993 [10], Penzien and Wu in 1998 [11], and Penzien in 2000 [12], that represent the so-called *soil–structure interaction approach*, based on the theory of an elastic beam on an elastic foundation, which takes into consideration the kinematic interaction effects in quasi-static conditions, but neglects the effects of dynamic interaction. A comprehensive review on all of these methods is given by Hashash et al. [13].

Considering that the dynamic FE analyses are quite complex and they require large computer capacities, the present study employs simplified dynamic analyses for both discrete and continuous models, performed with a view toward investigating the seismic response of tunnels. Such simplified methods cannot adequately simulate the earthquake-induced changes in ground stiffness and strength, and they ignore the inertial soil–structure interaction effects. Yet, these methods give a reasonable estimation of the seismic loads regarding an initial evaluation of strains and deformations in a tunnel [14].

In the examined study, two-dimensional coupled beam–spring as well as finite element models have been employed using the ANSYS software [15], to investigate the tunnel–ground interaction effects. The models have been subjected to the seismic load under simple shear conditions obtained by a one-dimensional seismic site response (SSR) analysis, which ignores the effects of the tunnel shape and stiffness on the seismic behaviour of the ground. In addition, the SSR analysis ignores the effects of compressional P-waves, since only shear S-waves, which propagate in vertical planes inducing soil shear strain, are considered. Taking advantage of two different modelling approaches – discrete and continuous – the SSI phenomenon has been analysed and the obtained results concerning both models are compared.
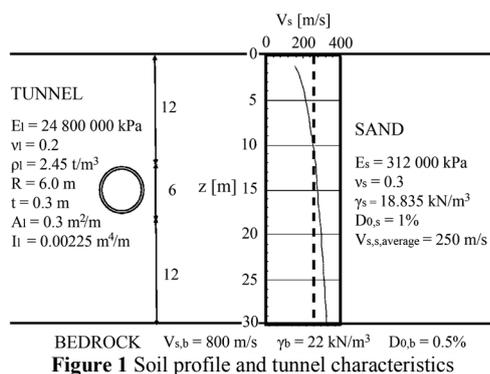
2 Ground conditions and tunnel characteristics

A circular tunnel structure, with the external tunnel radius of 3,0 m and the thickness of the liner of 0,3 m, is placed at the depth of 15 m in a dense sandy soil layer with the thickness of 30 m, which lies over a relatively stiff bedrock. The material properties of the liner and the ground are given in Fig. 1. The shear wave velocity profile $V_s(z)$ is also presented in the given figure, where the dashed line denotes an average value of the shear wave velocity within the soil layer. This value was required for the purpose of performing a one-dimensional linear analysis of the seismic response of the ground.

3 Description of the numerical models

In developing the analyses, the following assumptions are adopted:
- A region of the surrounding ground is considered as a homogeneous and isotropic half-space;
- Both the soil and the tunnel lining are treated as materials with elastic behaviour;
- Assuming uniform properties of the tunnel structure, the ground, and the loading along the tunnel's length, two-dimensional plane-strain analyses were conducted.

During an earthquake excitation, considerable static stresses, attributed to the overburden pressure and the construction process, are acting on the tunnel structure. For that reason, prior to the simplified dynamic analyses presented in this study, corresponding static analyses have also been performed, in order to check the models for static conditions as well.

3.1 Discrete coupled beam–spring model (ANSYS)

The ANSYS 2D discrete model consists of 36 two-nodded Timoshenko beam elements for the tunnel lining and two-nodded linear spring elements for the soil, placed in the radial (36 elements) and tangential directions (36 elements). At each node there are three DOF (U_x, U_y, ROT_z) for the beam and one DOF for the spring elements.

The main purpose of the spring elements is to model the soil–tunnel structure interaction by elastic supports as a discrete contact, simulated by a coupled-type interaction spring consisting of a radial ground spring and a tangential ground spring.
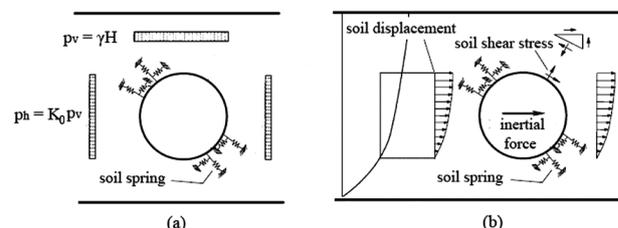

Figure 2 Discrete beam–spring model: (a) static analysis; (b) dynamic analysis

In the static analysis, the effect of tunnel–ground interaction is accomplished in the form of the elastic subsoil reaction distributed radially on a tunnel ring, i.e., the bedding zone. The modulus of the subsoil reaction depends on the soil–lining coupling being influenced by the type and properties of the soil, the shape and the

Figure 1 Soil profile and tunnel characteristics

dimensions of a structure, and the value of active loading. In practice, active loads are divided in vertical and horizontal direction (Fig. 2(a)). Yet, in reality, they act radially and tangentially on the curved shape of the circular tunnel surface. Therefore, in the given analyses, the active earth pressures have been calculated both in the radial and tangential directions.

The soil in the contact area could not be imposed to tension (in that case, there is no contact between the soil and the structure, and by that, no soil–structure interaction exists). This drawback has been overcome by elimination of the tensioned zone (i.e., tensioned soil springs) from the model (the area above the tunnel crown), along with the repetition of the calculating process.

The Seismic Deformation Method, which explicitly considers the seismic deformation of the ground, is based on the concept that seismic forces acting on the beam–spring model are assumed to be the result of earthquake induced ground displacements, ground shear stress, and inertial force [16], as illustrated in Fig. 2(b). The maximum relative displacement between the top and the bottom of the tunnel cross-section was considered throughout the analysis. The ground displacements obtained by 1D linear SSR analysis are applied through soil springs placed radially and tangentially to the tunnel section of the ANSYS's beam–spring model in a pure shear condition. The ground shear stress τ_{ave} in the range of depths between the tunnel crown and invert, computed also by 1D SSR analysis, has been applied directly to the lining. This method accounts for the behaviour of both soil and structure, and takes into consideration the kinematic tunnel–soil interaction effects approximately.

The analyses presented here were performed only for the no-slip condition, as it results in the extreme values of the thrust in the tunnel lining. The tied degrees of freedom boundary condition was applied at the contact between the tunnel lining and the surrounding ground-springs [17], in order to constrain the nodes of both beam and spring elements to deform identically for the purpose of no-slip condition simulation, assuming compatible displacements of the lining and the ground.

For the purpose of the given analyses, properties of soil springs have been determined after solutions given by a number of authors: St. John and Zahrah, 1987 [5], Matsubara and Hoshiya, 2000 [18], ALA-ASCE, 2001 [19], Verruijt, 2005 [20]. After conducting a series of numerical tests, the value of the soil spring stiffness, which was finally adopted in the analyses, was according to ALA-ASCE [19] ($K = 20\,567\,820$ N/m). It was the smallest obtained value for the soil spring constants, and the only one for which it was possible to successfully simulate the elastic subgrade reaction in the static analysis. In this way, the flexible surrounding medium was modelled, in which case the soil–tunnel interaction is the most pronounced and applying the springs in the model is meaningful. Thus, the chosen spring coefficient simulates the soil properly not only in static, but under dynamic conditions as well. The same spring stiffness is applied in the radial and tangential directions.

3.2 Continuous FE model (software ANSYS)

In the continuous FE model, the computational soil domain was modelled with the outer boundaries extending to a distance greater than four times the tunnel

diameter R, in order to minimise the boundary effects. The width of the model is selected to be 54 m ($4R+R+4R$). The height of the model is 30 m, which is in line with the thickness of the soil deposit over the bedrock. The ANSYS free-meshing algorithm was applied to obtain a high quality spatial discretisation. The mesh was refined around the tunnel, in areas of high stress concentration, in order to increase the accuracy of the analysis (Fig. 3).
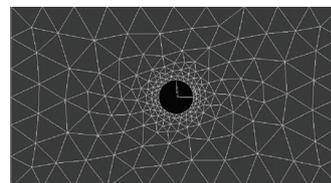

Figure 3 Continuous FE model for static and dynamic analysis

The ground was modelled by plane strain solid elements and the tunnel was modelled by beam elements. At each node there are two DOF (U_x, U_y) for the plane elements, and three DOF (U_x, U_y, ROT_z) for the beam elements. The FE mesh consists of 368 six-nodded triangular solid elements and 36 two-nodded beam elements, without using any interface elements. The tied degrees of freedom boundary condition was applied along the conjunctive surface of the tunnel and the ground. This boundary condition constrains nodes on the two sides of dissimilar meshes to deform identically assuming compatible displacements of the lining and the ground, for the purpose of the no-slip condition simulation.

The displacements in both directions are fixed at the bottom of the model, thus simulating the rigid bedrock under the soil layer. The upper horizontal boundary of the FE model is considered to be free, as it simulates the ground surface. In the static analyses, roller supports along the vertical boundaries have been used to restrict horizontal displacements, whereas in the dynamic analyses vertical displacements were restricted along the side boundaries. In the full FE analyses (with simultaneously combined static and dynamic influences), both vertical and horizontal displacements were allowed at the vertical boundaries of the model.

3.3 One-dimensional SSR analysis (code EERA)

The one-dimensional site response analyses have been carried out by means of the code EERA [21], in which the solution of wave propagation equations is done in the frequency domain.
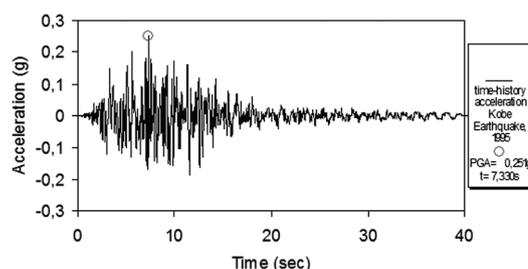

Figure 4 Acceleration record used in 1D SSR analysis

In the present analyses, ground conditions were modelled according to Fig. 1. The free-field ground deformations induced by the seismic wave propagation

are calculated by assuming a linear elastic behaviour of the soil, which implicates that the soil shear modulus and damping coefficient are constant throughout the analysis and do not depend on a level of shear strains.

Fig. 4 illustrates the acceleration time history of the 1995 Kobe Earthquake in Japan, employed in all dynamic SSR analyses. These earthquake data were used, since this earthquake event was the most devastating to civil infrastructure in recorded history. Due to the scarcity of bedrock strong motion records in the vicinity of tunnels, the surface accelerogram was scaled to $0{,}25 \cdot g$ ($2{,}46$ m/s^2) to account for strong motion attenuation with depth [22]. The peak value of the input acceleration time history appears approximately $7{,}3$ s after the onset of the excitation. The acceleration input is applied to the bottom boundary of the soil column model (rigid bedrock).

Earthquake-induced acceleration, shear stress, and strain at the tunnel depth were calculated by a free-field one-dimensional SSR analysis (Fig. 5). As the bedrock is rigid, it acts as a fixed end boundary, by which all downward-travelling waves in the soil layer overlying the bedrock are completely reflected back toward the ground surface and all of the elastic wave energy is trapped within the soil layer. This has resulted in somewhat higher value of γ_{max} in the linear analysis, and it is considered that the rigid-bedrock approach is not applicable to real soil.

The value γ_{ave}, as the design free-field shear strain of the soil in the seismic analysis of tunnel structures [23], representing the average soil shear strain in the range of depths between the tunnel crown and the invert, and the corresponding soil shear stress τ_{ave} have been calculated.
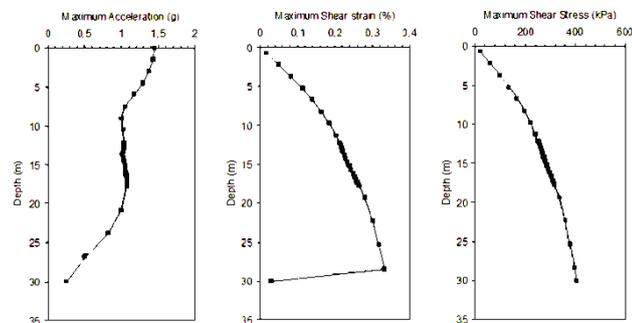

Figure 5 Maximum acceleration, shear strain, and shear stress profiles obtained by the 1D SSR linear analyses

In the discrete beam–spring model, the calculated soil displacements induced by an earthquake excitation are then applied through the soil springs to the tunnel section in a pure shear condition, whereas the soil shear stress (τ_{ave}) was applied directly to the tunnel lining. In the continuous FE model, the obtained seismically induced soil displacements are then applied to the vertical side boundaries of the model in a simple shear condition. By that, both the acceleration time history and the site characteristics are taken into account, considering the kinematic tunnel–soil interaction effects. However, the dynamic soil–structure interaction is ignored.

Lastly, the numerical analysis results have been compared with closed-form elastic solutions, based on the most frequently used analytical expressions for evaluation of earthquake-induced stress increment in a tunnel lining by taking into consideration the soil–structure interaction

effects. These expressions are given in terms of the design shear strain field γ_{ave} [24], which is the cause of the ovalisation of the circular tunnel cross-section.

4 Discussion on the results
4.1 Comparison of the numerical dynamic analysis results and closed-form elastic solutions

In order to compare the obtained numerical results regarding the simplified dynamic linear analyses, the analytical solutions after Wang, 1993 [10] and Penzien, 2000 [12] have been used. The internal forces in the lining have been calculated from the free-field shear strain obtained by the code EERA. Under the assumption of the perfect contact between the tunnel and the ground (i.e., compatible displacements of the lining and the soil), the variation of accumulated thrust (N), shear force (T), and bending moment (M) in terms of the angle θ is calculated according to expressions given by the aforementioned authors, whereby the angle θ is measured counter clockwise with respect to the horizontal axis.
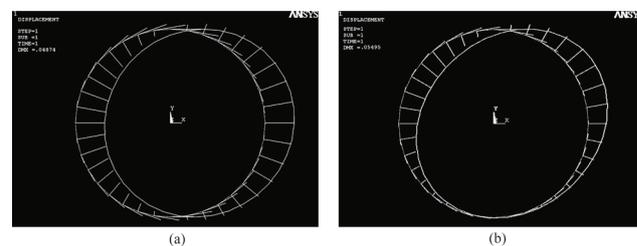

Figure 6 Different ovaling deformation shapes of the circular tunnel cross-section: (a) beam–spring model without soil shear stress; (b) beam–spring model accounting for soil shear stress

In applications of the beam–spring model, conducting a simplified dynamic analysis in a simple shear condition, it is quite usual to take into account only the earthquake induced displacements and tunnel section inertial force, without considering the influence of soil shear stress. In relation to that, the two cases have been analysed in the present study: a beam–spring model without considering the seismically induced soil shear stress (Fig. 6(a)) and a beam–spring model that involves the soil shear stress (Fig. 6(b)), in order to estimate the error when the shear stress of the soil medium is not accounted for. The common conclusion that can be drawn regarding all the forces in the tunnel lining is that excluding the soil shear stress from the coupled beam–spring model, in order to simulate SSI effects, leads to a significant underestimation of the internal lining forces (Fig. 7).

The dynamic analyses have simulated the ovaling deformation pattern of the circular tunnel cross-section successfully, since the extreme values of the thrust and bending moment occur at the shoulder and knee locations, i.e., tunnel soffits (at $\theta = 45°$, $135°$, $225°$, and $315°$), whereas the maximum values of the shear force are observable at the tunnel crown, abutments, and invert regions (at $\theta = 0°$ ($360°$), $90°$, $180°$, and $270°$) (Fig. 7).
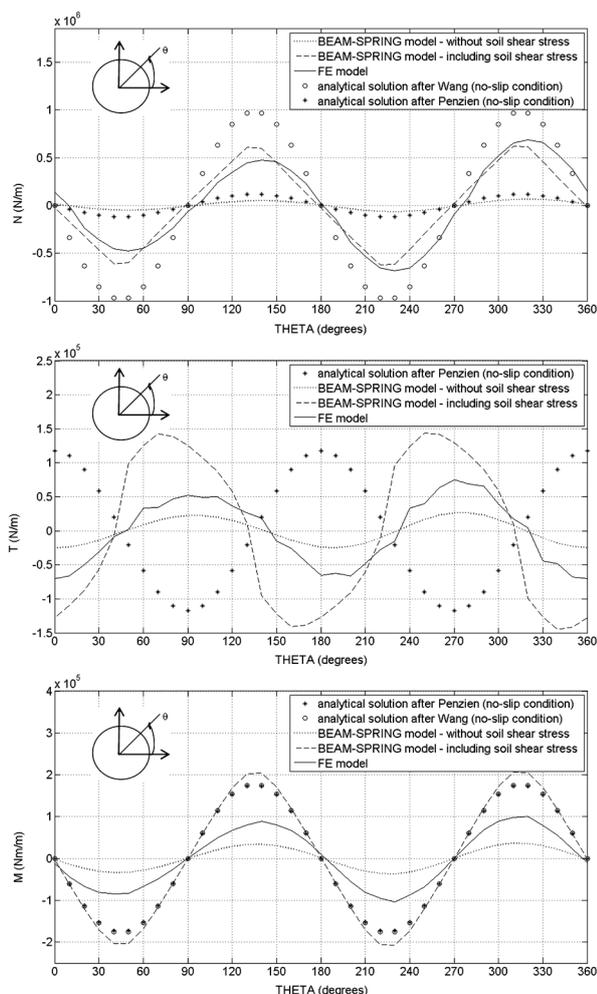
Figure 7 Comparison of numerical dynamic analysis results with analytical solutions after Wang, 1993 [10] and Penzien, 2000 [12]

4.1.1 Seismically induced thrust in the tunnel lining

With regard to the earthquake-induced thrust distribution along the tunnel lining, referring to the aforementioned figure (Fig. 7), both the beam–spring model, when accounting for the soil shear stress, and the FE model provide fairly consistent distribution of *N*-force, whose maximum values are slightly lower in comparison with the Wang's solution [10]. This is in accordance with the conclusion that seismically induced thrust tends to increase with decreasing the compressibility and flexibility ratios of the ground relative to the tunnel lining [13]. Therefore, the reason for the inconsistency of the analytical and numerical results regarding the maximum values of thrust is that the ground conditions considered in the given analyses are of better characteristics (medium dense sand), and thus with the higher compressional and shearing stiffness. The corresponding conclusion that may be drawn is that the expression of Wang for seismically induced thrust in a tunnel lining is better correlated to poorer soil properties with the lower compressional stiffness, such as loose sand or water-saturated undrained clay.

On the other hand, the beam–spring model without soil shear stress consideration highly underestimates the values of accumulated thrust, approximately the same as obtained by the Penzien's approach [12]. This observation confirms the conclusions that in the case of no-slip condition the Penzien's solution predicts much lower

thrust values than those predicted by the Wang's solution [25]. The reason for this underestimation is not clearly examined so far, but may be sought in the fact that the corresponding compressibility coefficient in the Penzien's expression for the seismically induced lining thrust for the no-slip condition is not introduced. In the Wang's expression for the tunnel lining thrust under the perfect tunnel-ground contact conditions, along with the flexibility ratio that stands for the ability of the structure to resist distortion imposed by the ground, the compressibility ratio that reflects the circumferential stiffness of the system, i.e. resistance to compression, is also taken into account. In the Penzien's expression for the earthquake-induced tunnel lining thrust under the no-slip condition, however, only the flexibility ratio is taken into consideration. For that reason, it is recommended that in evaluation of the earthquake-induced tunnel lining thrust the Penzien's analytical solution given for the no-slip condition should be avoided [24].

Accordingly, ignoring the soil shear stress in a simplified dynamic analysis by using a beam–spring model yields an error which could not be tolerated, since a contact between a structure and a surrounding ground in the model is defined in a discrete manner, only at a number of points, in contrast to a FE model, in which case the soil–structure interface is continuous, around the entire external lining surface.

Referring to all of the previously mentioned, it could be concluded that in order to develop reliable simulations and obtain relevant results, a beam–spring model in a simplified dynamic analysis should take into consideration, besides the earthquake induced soil displacements and the tunnel inertial force, also the soil shear stresses.

4.1.2 Seismically induced shear forces and bending moments in the tunnel lining

The distributions of shear forces and bending moments along the tunnel lining according to the analytical and numerical results are also illustrated in the same plots (Fig. 7). The presented distribution of shear forces is opposite to the Penzien's solution, since in the ANSYS software the opposite sign convection for *T*-forces is established. With regard to the earthquake-induced shear forces and bending moments, the discrete beam–spring models involving soil shear stress for the no-slip assumption predict distribution that matches quite well with the solutions according to Penzien and Wang. This is opposite to the discrete models that do not account for soil shear stress, in which case shear force and bending moment values are significantly underestimated when compared with the elastic closed-form solutions. On the other hand, the results of the FE model are somewhat smaller than those obtained by the closed-form elastic solutions.

This is exactly the point where the significance of the soil–structure interaction effects becomes pronounced. Namely, there is an evident difference between the free-field ground deformation and the deformation of a ground with tunnel structure in it. In the case of the discrete beam–spring model, earthquake induced displacements, calculated by EERA code (neglecting the effects of the tunnel shape and stiffness on the seismic response of the ground), have been applied through soil springs directly to the tunnel structure, which has resulted in the higher

values of shear forces and bending moments in the liner. In the continuous FE model, however, the calculated free-field displacements have been applied along the side boundaries of the model, in which case both the soil stiffness and the tunnel structure stiffness have played an important role in the coupled tunnel–ground seismic behaviour: the soil shearing stiffness in transmitting the seismically induced displacements from the far-field to the tunnel section, and the flexural stiffness of the tunnel cross-section in impeding the development of the free-field motion, thus resulting in the lower values of shear forces and bending moments in the tunnel lining.

Accordingly, it can be concluded that, unlike the discrete beam–spring models, the continuous FE models comprehensively demonstrate the importance of the kinematic soil–structure interaction effects. Considering the former stated remarks, as well as the fact that the shear force and bending moment maximum values computed by the FE model are somewhat smaller than those obtained by the closed-form elastic solutions, it seems that the expressions of Wang and Penzien are better correlated to poorer soil properties with the shearing stiffness lower than that of the dense sandy soil considered throughout the given analyses.

Finally, it may be observed that the magnitude of thrust has a much stronger influence than moments over the stresses accumulated in the tunnel lining, which is in accordance with the no-slip condition assumption.

The obtained dynamic analysis results have revealed that the relative contribution of the tunnel section inertial force in the total of internal lining forces is far below 1%. This is not surprising, since the tunnel section inertia is negligible relative to the inertia of the surrounding ground. Therefore the inertial forces could be considered to be negligible.

4.2 Comparison of the models regarding the influence of static, dynamic, and total loading upon the internal lining forces

4.2.1 Lining force distributions under static, dynamic, and total loading (discrete beam–spring model)

In the case of the beam–spring model it is not possible to analyse both static and dynamic effects simultaneously, in order to examine a relative contribution of an initial static loading in internal lining forces under dynamic conditions. This is referred to a symmetrical nature of the static loading and anti-symmetrical fashion of the dynamic one. In developing the static analyses, namely, there was a necessity to eliminate tensioned radial soil springs, in order to make a model being able to simulate realistic conditions, whereas in the dynamic analyses the same radial springs have been loaded by compression. Therefore, the only possible solution in that situation is to superimpose seismic effects onto the static initial conditions.

As it could be seen from the superimposed static and dynamic analysis results regarding the beam–spring model (Fig. 8), superposition of the given effects shows that the total internal lining forces follow the distribution pattern typical for dynamic influences, thus implying the domination of dynamic loads over the static ones, which is consistent with the real physical state. When it comes to the sign of these forces, however, there is a noticeable discrepancy between the obtained numerical results

regarding the dynamic analysis and the analysis with superimposed effects, which is particularly evident for the case of the thrust distribution. Unlike the alternating nature of the thrust distribution under dynamic loads, the analyses with superimposed effects imply on the predominantly compressed tunnel lining, which is typical under static conditions.
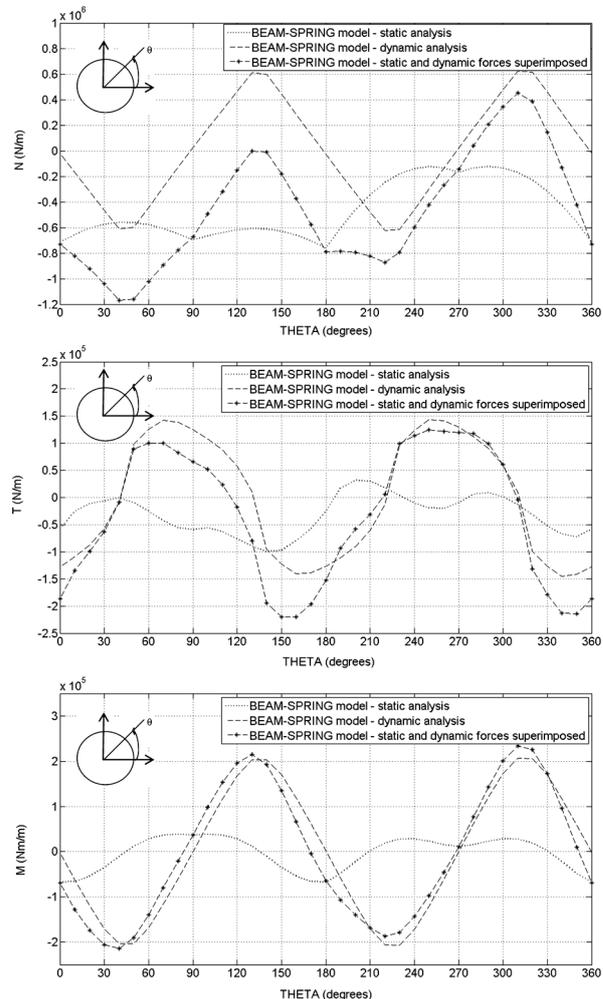

Figure 8 Numerical results of the lining force distributions under static, dynamic, and superimposed effects using the beam–spring model

4.2.2 Lining force distributions under static, dynamic, and total loading conditions (continuous FE model)

Unlike the beam–spring model, static and dynamic effects using the continuous FE model have not been superimposed, but both effects have been simultaneously combined within the single (full) numerical analysis.

The results reported in the attached diagrams (Fig. 9) imply that dynamic effects completely dominate the lining force distributions under total loading conditions, both from the aspect of the distribution pattern coincidence (the cosine form of thrust and bending moments, and the sine form of shear forces), and from the aspect of the quite good agreement of the force signs and sections where the extreme force values appear.
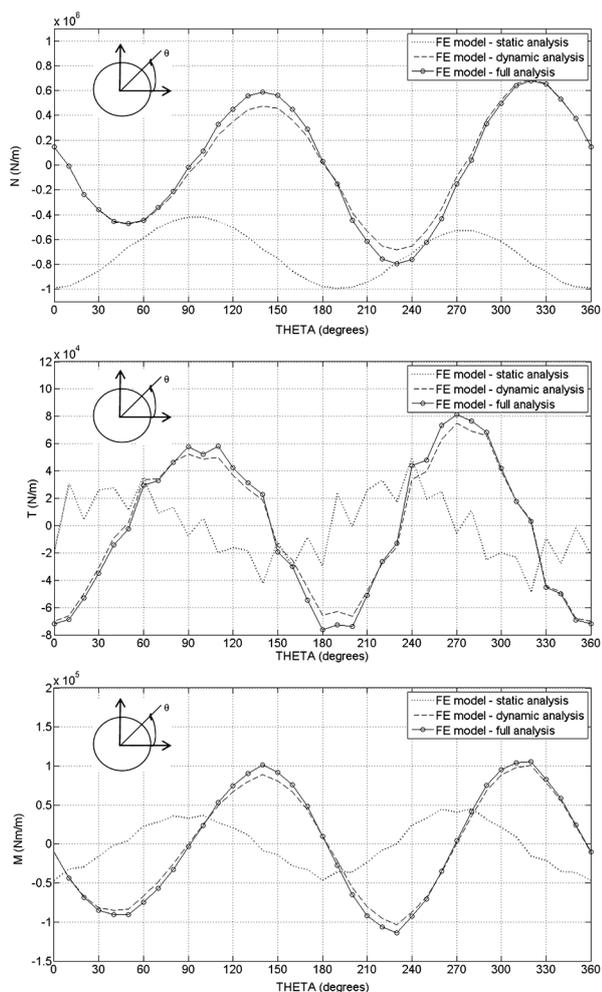
Figure 9 Numerical results of the lining force distributions under static, dynamic, and total loading conditions using the continuous FE model

4.2.3 Discrete beam–spring vs. continuous FE model

Comparing the results of the total lining force distribution obtained by the beam–spring and FE models (Fig. 10), it is evident that the simple superimposing of the static and dynamic analysis results does not yield a correct solution in a comprehensive way. The general conclusion that can be drawn from the given diagrams is that the beam–spring model overestimates noticeably all the forces accumulated in the tunnel lining. In addition, considering the distribution of accumulated thrust, although the cosine distribution form and sections around the lining where stress concentrations appear are satisfied, the extreme values differ significantly in the cases of the beam–spring model superposition and full FE analysis. The analyses with the superimposed effects imply that the compressed nature of the tunnel lining, typical under static conditions, is predominant under dynamic conditions as well. This is not in a good agreement with the real physical state, since an earthquake excitation imposes the alternating compressive and tensile lining thrust distribution, which, on the other hand, is being confirmed by the full FE analysis.

In conclusion, a comprehensive FE analysis that includes simultaneously analysed effects of static and dynamic loading is always a better alternative, since it leads to much more accurate results related to the sign as

well as the distribution pattern of internal forces induced in a tunnel lining.
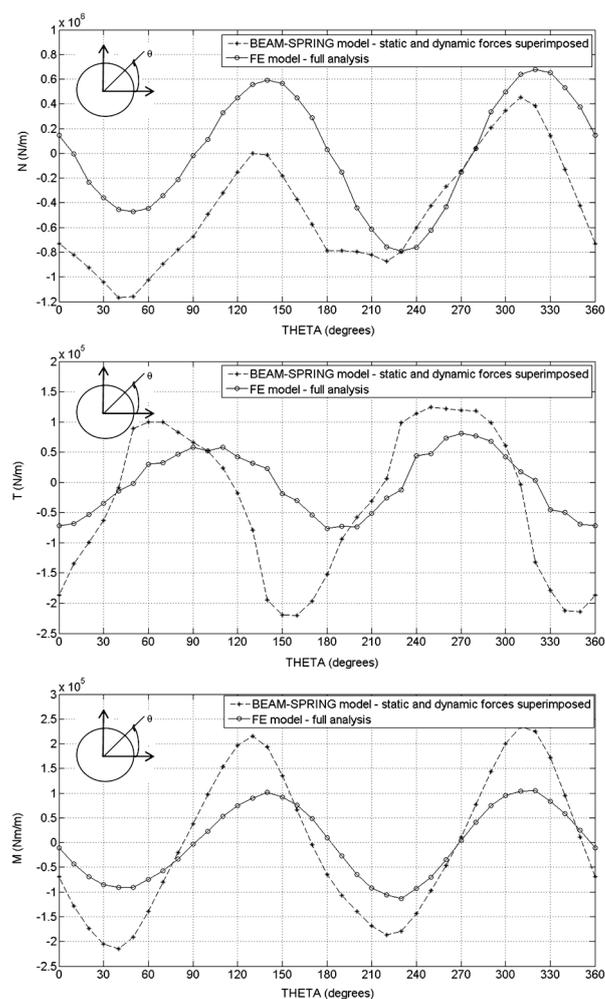

Figure 10 Comparison of the models regarding the lining force distributions under total loading

5   Concluding remarks

The analyses described in this paper, related to the soil – tunnel structure interaction phenomenon studied by discrete beam–spring and continuous FE models under static, dynamic, and total loading conditions, suggest the following conclusions:

-    Both coupled beam–spring and FE models allow simulation of the soil–tunnel structure interaction. For a beam–spring model soil spring coefficients should be chosen in such a way as to make a model being able to simulate soil properties successfully both under static conditions (elastic subgrade reaction) and under dynamic conditions (soil–tunnel structure interaction);

-    When using the beam–spring model, in order to simulate the SSI effects correctly, soil shear stresses should be taken into account along with earthquake induced displacements, whereas the tunnel section inertial force could be considered to be negligible, since its relative contribution in the total of internal lining forces is far less than 1 %;

-    Continuous FE models take into consideration the kinematic soil–structure interaction effects thoroughly, in much more accurate and proper way in comparison with beam–spring models, as they account both for a soil

shearing stiffness in transmitting seismically induced displacements from a far-field to a tunnel section, and for a flexural stiffness of the tunnel cross-section in impeding the development of the free-field ground motion;

- A significant discrepancy in magnitudes of the seismically induced tunnel lining thrust computed after the Wang's and Penzien's expressions is observed. The comparisons with the numerical results clearly indicate that the Wang's expression provides a realistic evaluation of the lining axial force for the perfect tunnel–ground interface condition. Consequently, the Penzien's solution for earthquake-induced thrust in the tunnel lining under the no-slip condition assumption should be avoided;

- Unlike the beam–spring model that cannot analyse static and dynamic effects simultaneously except by simple superposition, the continuous FE model allows to account both for static and dynamic loads in a single analysis. The simple superimposing of the results given by uncoupled static and dynamic analyses using the beam–spring modelling approach does not lead to the correct solution in a comprehensive way. This is particularly true for a distribution of the accumulated thrust, in which case, although the cosine distribution pattern is satisfied, the sign of forces as well as their extreme values differ significantly in comparison with the results of analyses using the continuous FE modelling approach. Unlike the FE analyses that result in the alternating compressive and tensile lining thrust distribution under total loading conditions, the analyses with superimposed static and dynamic effects imply that the compression loading in a tunnel lining, typical for initial static conditions, is predominant under dynamic conditions as well, which is not in a good agreement with the real physical state.

Acknowledgements

6   References

[1] Cerić, A.; Marčić, D.; Ivandić, K. A risk-assessment methodology in tunnelling. // Technical Gazette. 18, 4(2011), pp. 529-536.

[2] Kouretzis G. P.; Sloan, S. W.; Carter, J. P. Effect of interface friction on tunnel liner internal forces due to seismic S- and P-wave propagation. // Soil Dynamics and Earthquake Engineering. 46, (2013), pp. 41-51. DOI:10.1016/j.soildyn.2012.12.010

[3] Owen, G. N.; Scholl, R. E. Earthquake engineering of large underground structures. Report FHWA/RD-80/195, Federal Highway Administration and National Science Foundation, McLean, Virginia, 1981.

[4] Newmark, N. M. Problems in wave propagation in soil and rock. // Proceedings of the International Symposium on Wave Propagation and Dynamic Properties of Earth Materials / Albuquerque, New Mexico, 1968, pp. 7-26.

[5] St. John, C. M.; Zahrah, T. F. Aseismic design of underground structures. // Tunnelling and Underground Space Technology. 2, 2(1987), pp. 165-197. DOI: 10.1016/0886-7798(87)90011-3

[6] Burns, J. Q.; Richard, R. M. Attenuation of stresses for buried cylinders. // Proceedings of the Symposium on Soil–Structure Interaction / Arizona, 1964, pp. 378-392.

[7] Hoeg, K. Stresses against underground structural cylinders. // Journal of the Soil Mechanics and Foundations Division, ASCE. 94, 4(1968), pp. 833-858.

[8] Peck, R. B.; Hendron, A. J.; Mohraz, B. State of the art in soft ground tunnelling. // Proceedings of the Rapid Excavation and Tunnelling Conference / New York, 1972, pp. 259-286.

[9] Schwartz, C. W.; Einstein, H. H. Improved design of tunnel supports: vol. 1 – simplified analysis for ground–structure interaction in tunneling. Report UMTA-MA-06-0100-80-4, US Department of Transportation, Urban Mass Transportation Administration, Washington DC, 1980.

[10] Wang, J. N. Seismic Design of Tunnels: A State-of-the-Art Approach. Monograph, monograph 7. Parsons, Brinckerhoff, Quade and Douglas, Inc., New York, 1993.

[11] Penzien, J.; Wu, C. Stresses in linings of bored tunnels. // International Journal of Earthquake Engineering and Structural Dynamics. 27, 3(1998), pp. 283-300. DOI:10.1002/(SICI)1096-9845(199803)27:3<283::AID-EQE732>3.0.CO;2-T

[12] Penzien, J. Seismically induced racking of tunnel linings. // International Journal of Earthquake Engineering and Structural Dynamics. 29, 5(2000), pp. 683-691. DOI: 10.1002/(SICI)1096-9845(200005)29:5<683::AID-EQE932>3.0.CO;2-1

[13] Hashash, Y. M. A.; Hook, J. J.; Schmidt, B.; Yao, J. I.-C. Seismic design and analysis of underground structures. // Tunnelling and Underground Space Technology. 16, (2001), pp. 247-293. DOI: 10.1016/S0886-7798(01)00051-7

[14] Kontoe, S.; Zdravkovic, L.; Potts, D. M.; Menkiti, C. O. Case study on seismic tunnel response. // Canadian Geotechnical Journal. 45, (2008), pp. 1743-1764. DOI:10.1139/T08-087

[15] ANSYS Documentation, ANSYS Multiphysics. // Canonsburg, Pennsylvania (2012). http://www.ansys.com.

[16] Mizuno, K.; Koizumi, A. Dynamic Behavior of Shield Tunnels in the Transverse Direction Considering the Effects of Secondary Lining. // Proceedings of the 1st European Conference on Earthquake Engineering and Seismology / Geneva, Switzerland, 2006, Paper No. 1359.

[17] Zlatanović, E.; Broćeta, G.; Popović-Miletić, N. Numerical modelling in seismic analysis of tunnels regarding soil–structure interaction. // Facta Universitatis, Series: Architecture and Civil Engineering. 11, 3(2013), pp. 251-267. DOI:10.2298/FUACE1303251Z

[18] Matsubara, K.; Hoshiya, M. Soil spring constants of buried pipelines for seismic design. // Journal of Engineering Mechanics, ASCE. 126, 1(2000), pp. 76-83. DOI: 10.1061/(ASCE)0733-9399(2000)126:1(76)

[19] ALA-ASCE. Guidelines for the Design of Buried Steel Pipe. // Reston, Virginia (2001). http://www.americanlifelinesalliance.org. (13.02.2013).

[20] Verruijt, A. Soil Dynamics. Delft University of Technology, Delft, Netherlands, 2005.

[21] Bardet, J. P.; Ichii, K.; Lin, C. H. EERA – A computer program for Equivalent-linear Earthquake site Response Analyses of layered soil deposits. // University of Southern California, Los Angeles, California (2000).

[22] Kramer, S. L. Geotechnical Earthquake Engineering. Prentice Hall, New Jersey, 1996.

[23] Zlatanović, E.; Lukić, D.; Šešov, V. Pseudo-static and simplified dynamic methods of design soil shear strain evaluation in seismic analysis of tunnel structures. // Izgradnja. 68, 1-2(2014), pp. 9-19, (in serbian).

[24] Zlatanović, E.; Lukić, D.; Šešov, V. Presentation of analytical solutions for seismically induced tunnel lining forces accounting for soil–structure interaction effects. //

Building Materials and Structures. 57, 1(2014), pp. 3-28. DOI:10.5937/grmk1401003Z

[25] Hashash, Y. M. A.; Park. D.; Yao, J. Ovaling deformations of circular tunnels under seismic loading: an update on seismic design and analysis of underground structures. // Tunnelling and Underground Space Technology. 20, (2005), pp. 435-441. DOI:10.1016/j.tust.2005.02.004

Authors' addresses

Elefterija Zlatanović, PhD, Assistant
University of Niš, Faculty of Civil Engineering and Architecture
Aleksandra Medvedeva 14, 18000 Niš, Serbia
E-mail: elefterija2006@yahoo.com

Vlatko Šešov, PhD, Full Professor
University "Ss. Cyril and Methodius" of Skopje
Institute of Earthquake Engineering and Engineering Seismology
Todor Aleksandrov 165, 1000 Skopje, Republic of Macedonia
E-mail: vsesov@gmail.com

Dragan Č. Lukić, PhD, Full Professor
University of Novi Sad, Faculty of Civil Engineering of Subotica
Kozaračka 2a, 24000 Subotica, Serbia
E-mail: drlukic.lukic@gmail.com

Aleksandar Prokić, PhD, Full Professor
University of Novi Sad, Faculty of Civil Engineering of Subotica
Kozaračka 2a, 24000 Subotica, Serbia
E-mail: aprokic@eunet.rs

Marina Trajković-Milenković, PhD, Assistant
University of Niš, Faculty of Civil Engineering and Architecture
Aleksandra Medvedeva 14, 18000 Niš, Serbia
E-mail: trajmarina@gmail.com